A CFD Study on the Characteristics of Impinging Jet Flow on an H-type Beam

Gong Hee Lee *
Reactor System Department, Korea Institute of Nuclear Safety, Daejeon, 34142, Korea

Corresponding author: ghlee@kins.re.kr

***Keywords :** computational fluid dynamics, H-type beam, high-energy pipe rupture, jet impingement

1. Introduction

Impinging jet flows from the high-energy pipe rupture are characterized by the formation of a stagnation region, the presence of shock-wave structures, and intense turbulence generation, followed by a transition into laterally deflected wall-jet flows. As a result, significant fluctuating loads may be imposed on adjacent safety-related structures or components. In particular, for compressible jet flows, total pressure losses associated with shock-cell structures and turbulent dissipation may exert coupled effects on local impingement loads and overall flow stability.

In practical nuclear power plant environments, target objects are not limited to simple flat plates but often consist of complex geometrical features such as stiffeners, beams, and ribs. These geometrical characteristics can alter the size and location of the stagnation region, the spreading behavior of the bifurcated wall-jet flow, and the associated recirculation and separation structures, thereby directly influencing the magnitude and distribution of impingement forces and loads. Therefore, it is necessary to establish an engineering basis for the design of appropriate protective measures by quantitatively comparing and analyzing the coupled characteristics of the flow field (for examples, Mach number, turbulent kinetic energy, and total pressure) distributions and the corresponding impingement responses depending on the target geometry. In this context, the present study explains the characteristics of the impinging jet flow depending on the distance from the nozzle exit to the target H-type beam.

2. Analysis Model

Fig. 1 presents a schematic diagram of the analysis model in which the circular impingement plate used in the Marviken impinging jet test facility [1] is replaced with an H-type beam. The analysis model consists of a nozzle, a downstream pipe spool, and an H-type beam. To reduce computational cost, a symmetric jet-flow assumption was applied with respect to the central plane of the computational domain. The nozzle diameter (D) and length (L) were set to 0.509 m and 1.18 m, respectively.

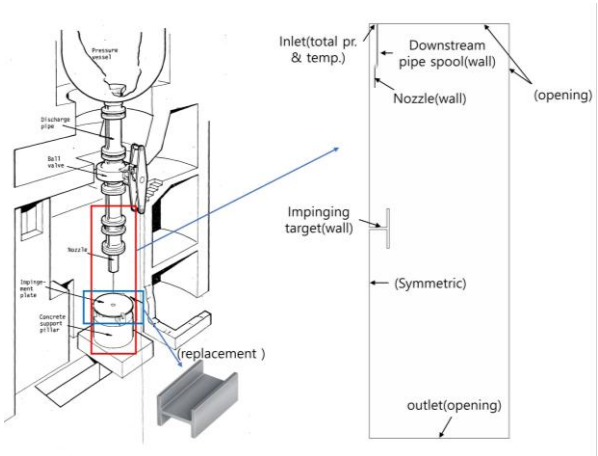

Fig. 1. Analysis model: computational domain & boundary conditions [1].

To investigate the characteristics of the impinging jet flow depending on the distance from the nozzle exit to the target H-type beam (L_p), numerical simulations were performed for four cases (L_p = 6.038, 6.942, 7.850, and 8.755 m). The computational domain was extended to 20.68 m in the axial direction and 7 m in the radial direction. It should be noted that additional simulations were attempted for L_p magnitudes shorter than 6.038 m; however, converged solutions could not be obtained. This may be attributed to the dominance of unsteady flow behavior in the corresponding configuration of the analysis model.

3. Numerical Modeling

The impinging jet flow was assumed to be steady, compressible, turbulent, and single-phase. For reference, the numerical methods and boundary conditions adopted in this study are summarized in Table I. The pressure and temperature measured at t=50 s, when only steam flow was present, were imposed as inlet boundary conditions.

Hexahedral elements were generated using ICEM-CFD. A total of approximately 7.02×10^5 elements was employed in the simulations. To accurately capture the jet flow and associated shock structures, a refined mesh was applied near the above-mentioned critical regions, including the nozzle exit, shock wave region, and adjacent wall surfaces. This meshing strategy is generally recommended for high-speed jet flow simulations.

Table I: Numerical methods and boundary conditions for flow analysis

Numerical methods		**Note**
Discretization accuracy for convection term	Momentum eqn.	High resolution
	Turbulence eqn.	High resolution
Turbulence model		SST k-ω
Velocity-pressure coupling		Rhie Chow (4th order)
Real gas model		Peng-Robinson
Near wall treatment		Automatic wall treatment
Convergence criteria		$< 10^{-5}$
Boundary conditions		**Note**
Inlet	Total pressure (kPa)	925
	Total temperature (℃)	176.5
	Turbulence	medium intensity (5%)
Outlet		Opening
Top plane, Side plane		Opening
Center plane		Symmetric
Wall		No-slip & smooth wall

4. Results and Discussion

Regarding to the applicability of ANSYS CFX R212 to jet flow analysis, previous study [2] demonstrated that the calculated static pressure profile along the axial direction from the nozzle exit (for a free jet flow without an impingement plate) showed good qualitative agreement with the experimental data.

Fig. 2 shows the calculated Mach number distribution depending on the distance from the nozzle exit to the target (L_p). For all L_p conditions, a periodic arrangement of high-Mach-number regions, commonly referred to as shock cells, is formed along the jet centerline. Such shock-cell structures are a typical feature of compressible jets when the nozzle exit condition is not perfectly matched with the ambient pressure (i.e., over-expanded or under-expanded), or when Prandtl–Meyer expansion waves and compression shock waves are generated alternately within the jet. At the jet boundary, a shear layer develops due to the velocity difference between the jet and the surrounding stationary fluid. In general, as L_p increases, the shear layer develops and mixing accumulates along the jet trajectory. This enhanced mixing modifies the effective Mach number and momentum distributions upon reaching the impingement surface and may influence the thickness and spreading angle of the lateral wall jets (radial or bifurcating flows). In the vicinity of the upper surface of an H-type beam (impingement surface), the jet flow undergoes rapid deceleration, leading to the formation of a stagnation region. In this region, several dominant compressible-flow phenomena occur simultaneously, including a pressure rise associated with flow impingement (stagnation pressure formation), flow separation and recirculation around the stagnation zone, and an abrupt redirection of the flow from the axial to the lateral direction. As L_p increases, the spreading angle of the lateral wall jet tends to increase, indicating enhanced energy dispersion.

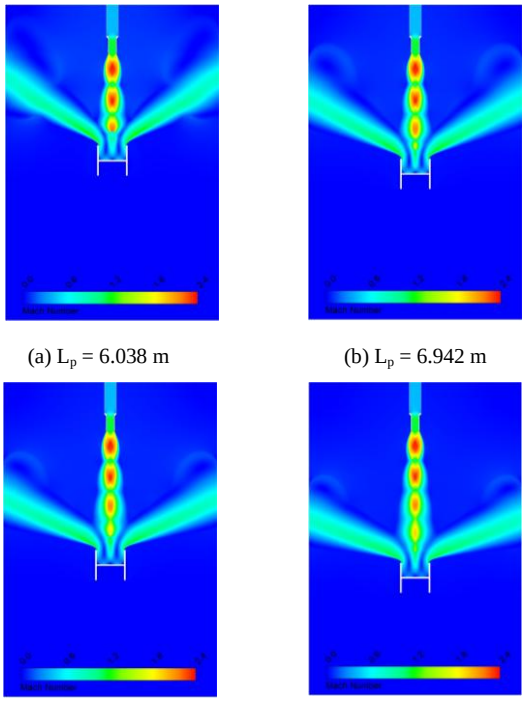

(a) L_p = 6.038 m (b) L_p = 6.942 m

(c) L_p = 7.850 m (d) L_p = 8.755 m

Fig. 2. The calculated Mach number distribution depending on the magnitudes of L_p.

Fig. 3 shows the distribution of turbulent kinetic energy (TKE) depending on the magnitudes of L_p. For all L_p conditions, the flow in the region where the jet impinges on the upper part of an H-type beam undergoes rapid deceleration and redirection. During this process, strong velocity gradients near the stagnation point, the pronounced pressure gradients, and the simultaneous occurrence of flow separation and recirculation lead to a peak in turbulent kinetic energy. Consequently, this region may represent the most vulnerable zone in terms of dynamic pressure fluctuations and fatigue loading. As L_p increases, the cumulative development of the shear layer prior to impingement results in an expansion of the high-TKE region near the impingement zone. In addition, turbulence generated at the impingement point is transported and diffused over a wider area along the downstream wall-jet.

Fig. 4 shows the total pressure distribution depending on the magnitudes of L_p. For all L_p conditions, a region of high total pressure is preserved along the jet centerline from the nozzle exit, indicating that the high-momentum flow discharged from the nozzle experiences relatively limited losses prior to impingement on the target. In addition, a periodic expansion and contraction pattern of the total pressure along the centerline—manifested as variations in the effective core thickness—is observed. This behavior corresponds to the shock-cell structure evident in the Mach number distribution, where repetitive local pressure fields are formed by alternating shock and expansion waves. During this process, cumulative total pressure losses are induced along the jet.

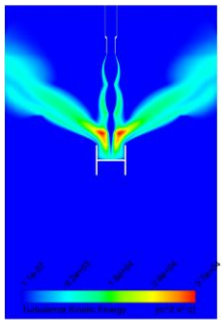
(a) L_p = 6.038 m

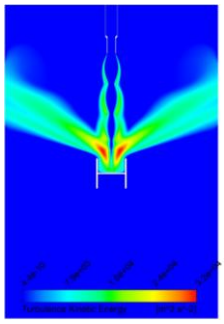
(b) L_p = 6.942 m

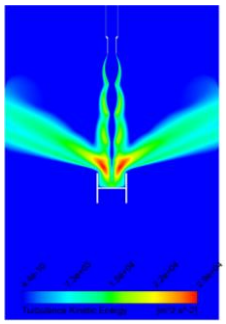
(c) L_p = 7.850 m

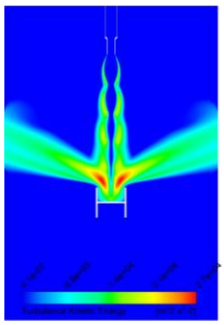
(d) L_p = 8.755 m

Fig. 3. The calculated turbulent kinetic energy distribution depending on the magnitudes of L_p.

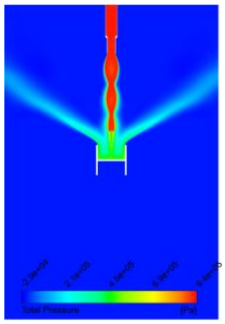
(a) L_p = 6.038 m

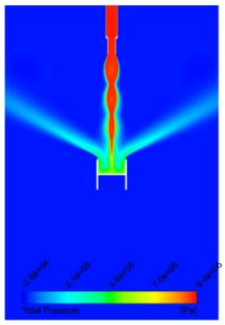
(b) L_p = 6.942 m

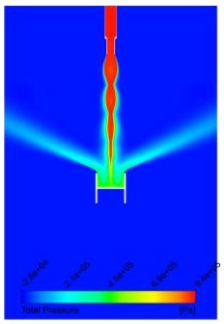
(c) L_p = 7.850 m

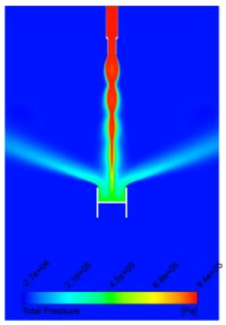
(d) L_p = 8.755 m

Fig. 4. The calculated total pressure distribution depending on the magnitudes of L_p.

Above an H-type beam, the free jet undergoes rapid deceleration and stagnation, resulting in pronounced changes in the total pressure field, including losses and redistribution. Downstream of the impingement region, the flow bifurcates laterally to form wall jets on both sides of the beam. Since this region has already experienced substantial losses, the total pressure within the wall-jet flow is reduced relative to that of the jet core and diffuses outward. As L_p increases, the extent of the loading and loss-affected region along the wall jet downstream of the impingement point tends to expand.

Fig. 5 shows the magnitudes of the horizontal and vertical forces acting on an H-type beam depending on the magnitudes of L_p. The acting force increased up to L_p = 6.942 m and subsequently decreased beyond this point. In general, as L_p increases, the jet flow undergoes shear-layer mixing, turbulent dissipation, and shock-related losses, resulting in a reduction in both total pressure and momentum. Consequently, the force acting on the target decreases with increasing L_p. However, when L_p is excessively short, the jet flow may impinge on the target before becoming fully developed. In such cases, the jet core remains overly contracted, and increased lateral spreading may occur prior to the conversion of momentum into stagnation pressure at the impingement surface, leading to a reduction in the force acting on the target. Conversely, as L_p increases to an intermediate range, the shear layer develops sufficiently, increasing the effective jet diameter at the impingement surface. This enhances the efficiency of momentum conversion into stagnation pressure upon the impact surface, thereby resulting in an increase in the force acting on the target.

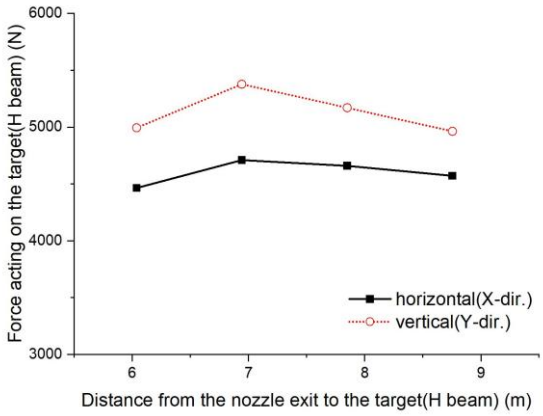

Fig. 5. Force acting on the target.

5. Conclusions

The distance from the nozzle exit to the target (L_p) is a governing parameter that controls the compressible-flow structure, turbulence generation, total pressure loss, and impingement load characteristics of the jet. The periodic shock-cell structures along the jet centerline promote cumulative shear-layer growth and mixing with increasing L_p, thereby modifying the effective Mach number and momentum distributions at the impingement surface. These changes lead to enhanced turbulent kinetic energy and redistribution of stagnation pressure in the impingement region and downstream wall-jet flow, ultimately resulting in a non-monotonic variation of the impingement force, with a peak occurring at an intermediate L_p. The present findings highlight the

coupled influence of jet development and target interaction on local and fluctuating loads and provide an engineering basis for determining appropriate separation distances and structural configurations to mitigate jet impingement loads in nuclear power plant applications.

DISCLAIMER

The opinions expressed in this paper are those of the author and not necessarily those of the Korea Institute of Nuclear Safety (KINS). Any information presented here should not be interpreted as official KINS policy or guidance.

ACKNOWLEGEMENT

This work was supported by the Korea Institute of Nuclear Safety (A3FD26030, A6FD26021 & A3EI25034).

REFERENCES

[1] Nuclear Energy Agency, The Marviken Full Scale Jet Impingements Tests: Test 5 Results, 1981, MXD-205.
[2] G.H. Lee, S.H. Choi, Preliminary CFD Study on Free Jet Flow at the Marviken Test Facility, Transactions of the Korean Nuclear Society Autumn Meeting, Oct. 30-31, 2025, Changwon, Korea.